International Journal of Hydrogen Energy 101 (2025) 887–903

Contents lists available at ScienceDirect

International Journal of Hydrogen Energy

journal homepage: www.elsevier.com/locate/he

Techno-economic analysis for the design of membrane reactors in a small-scale biogas-to-hydrogen plant

Michele Ongis [a,b,*], Mattia Baiguini [c,d], Gioele Di Marcoberardino [d], Fausto Gallucci [b], Marco Binotti [a,**]

[a] Politecnico di Milano, Dipartimento di Energia, Via Lambruschini 4a, 20156, Milano, Italy
[b] Sustainable Process Engineering, Department of Chemical Engineering and Chemistry, Eindhoven University of Technology, De Rondom 70, Eindhoven, 5612, AP, the Netherlands
[c] Scuola Universitaria Superiore IUSS, Palazzo del Broletto, Piazza Vittoria 15, Pavia, 27100, Italy
[d] Università degli studi di Brescia, DIMI – Dipartimento di Ingegneria Meccanica e Industriale, Via Branze 38, 25123, Brescia, Italy

ARTICLE INFO

Handling Editor: Ramazan Solmaz

Keywords:
Green hydrogen production
Biogas
Membrane reactors
Modelling
Techno-economic analysis

ABSTRACT

Pd-based membranes are a key-component to obtain high-purity hydrogen from gaseous mixtures. They can be integrated in reactors called Membrane Reactors (MR), where the selective removal of reaction products allows to circumvent equilibrium limitations of traditional reactors. MRs for hydrogen production from methane reforming have been already investigated in literature, where they showed potentialities in small-scale biogas plants. However, analyses have typically been performed fixing many operating conditions and geometrical parameters, while only investigating few of them. It is therefore difficult to generalize the conclusions and to have a clear overview of the process behaviour. This article proves that MR performance can be summarized in generalized performance charts, where it is possible to characterize the reactor and the overall MR-based system only based on the membrane area it contains, for each set of temperatures, pressures, feed composition, catalyst amount and steam-carbon-ratio. From techno-economic analysis, it turned out that LCOH is 6.81 €/kg for a system with 100 kg/day of hydrogen production at 20 bar, reaching 7.49 €/kg if compressed up to 700 bar. System performance have been compared with a traditional reactor followed by a PSA (LCOH = 7.31 €/kg), showing that MR-based solution outperforms benchmark for its higher capacity to separate hydrogen. A sensitivity analysis assessed the influence of major uncertain costs.

1. Introduction

Hydrogen economy is a relevant current topic in energy landscape [1]. It could support the decarbonization of several hard-to-abate sectors, by both its direct utilization in combustors and fuel cells and re-using it as feedstock for e-fuel production, where it can be more easily stored. Due to technical difficulties in its transportation, particularly interesting are the solutions that allows us an in-situ production of hydrogen. Among them, the green-H_2 pathway could be obtained starting from biogas.

BioGas (BG), a gaseous mixture mainly composed by methane and carbon dioxide, is typically produced starting from raw biomass through anaerobic digestion process. Biogas production in Europe have steadily increased [2] in recent years, and it is expected to further increase in the next years, as well as its production cost could drop significantly [3]. Hydrogen can be produced from biogas via reforming process, where methane reacts with water producing hydrogen, carbon dioxide and carbon monoxide, following the well-known steam reforming and water gas shift (WGS) reactions. Conventional reforming process consists of a high-temperature reforming reactor, followed by one or two WGS stages, and then hydrogen is separated typically through Pressure Swing Adsorption (PSA) [4]. However, PSA is typically not ideal as a small-scale solution, since it maintains consistent costs while reducing its hydrogen separation capacity [5].

A valid alternative can be represented by the adoption of Membrane Reactors (MRs), integrated unit operations where hydrogen selective membranes are immersed into a catalytic chemical reactor [6,7]. Among hydrogen selective membranes, dense metallic membranes, based on

* Corresponding author. Politecnico di Milano, Dipartimento di Energia, Via Lambruschini 4a, 20156, Milano, Italy.
** Corresponding author.
E-mail addresses: michele.ongis@polimi.it (M. Ongis), marco.binotti@polimi.it (M. Binotti).

https://doi.org/10.1016/j.ijhydene.2024.12.245
Received 11 September 2024; Received in revised form 13 December 2024; Accepted 14 December 2024
Available online 4 January 2025
0360-3199/© 2024 The Authors. Published by Elsevier Ltd on behalf of Hydrogen Energy Publications LLC. This is an open access article under the CC BY license (http://creativecommons.org/licenses/by/4.0/).

palladium alloys, have always gained a particular attention due to their high hydrogen permeability and very high perm-selectivity (i.e. selectivity to permeation of hydrogen compared to other molecules) [8]. In recent years, technical improvements allowed the production of coated Pd–Ag thin-film membranes, where a ceramic layer (about 1 μm) protects the selective Pd layer (about 4–5 μm) that is in turn deposited on a ceramic porous tube as a support for the membrane [9]. These membranes, known as double-skin, have been developed specifically for their application in Fluidized Bed Membrane Reactors (FBMRs), where they have been tested for long-term operations [10].

In the EU funded project MACBETH [11], MRs are developed at TRL7 for different applications. Among them, FBMR for hydrogen production from reforming are developed both in autothermal (ATR) and externally heated configurations, the former using biogas as feed and the latter using natural gas. This industrial interest in MR technology requires a deep dive knowledge of their design and off-design behaviour and operation. Therefore, modelling activity is an important support at this state to help filling the gap towards full industrial application.

Modelling of hydrogen permeation through Pd-based membranes is widely studied in literature [12], both focusing on their usage for hydrogen separation [13–15] and in membrane reactors [16,17]. MRs are studied as a single unit or integrated in an overall process model, not only for methane reforming but also alcohols reforming [18], dehydrogenation reactions [19] and decompositions [20–22].

Techno-economic assessment of MRs for hydrogen production from reforming have already been performed in literature [23,24]: both assessing system performance compared to benchmark solutions and investigating the influence of operating conditions [25], investigating the usage of different feedstocks (e.g. biomethane) [26], including carbon capture [27] or focusing on energy efficiency [28]. This work also performs a techno-economic assessment of a MR-based system for hydrogen production. However, compared to the previous analyses, a preliminary study is done on the MR to understand the effect of each parameter on its performance. A deep understanding of the reactor performance allows to avoid techno-economic investigations in different conditions that have equivalent results from an energy balance viewpoint.

Accordingly, in this work, all relevant parameters are listed and their influence is investigated in the process of hydrogen production from biogas autothermal reforming. Considerations start at reactor level, where the reactor geometry, the membrane area distribution, and the fluidization velocity, in relation with the feed flow rate, are studied. This procedure allows us to reduce the number of parameters that should be investigated in the techno-economic and, moreover, allows us to have a broad picture of the overall system behaviour. In techno-economics, a sensitivity on major costs allows to define scenarios, as well as a comparison with benchmark is included and an analysis on how reactor temperature and pressure affects costs and performance.

2. Modelling, methodology and assumptions

2.1. Membrane reactor: FBMR model and performance charts

The FBMR model used in this work has been developed by Foresti et al. [29], and its detailed description can be found in Ongis et al. [30]. Only the primary features of the model are hereby reported. It is a 1D two-phases continuous model, where material balances for all species involved are solved and an overall energy balance is performed to verify the autothermal behaviour of the reactor. It has been developed in Aspen Custom Modeler® (ACM) software, to be easily integrated in Aspen Plus® for system calculations. The equations of the mathematical model describe the fluid dynamics of the fluidized bed, the permeation through the dense metallic membranes and the material and energy balances. The involved chemical reactions are the methane steam reforming (R.1), the water gas shift (R.2) and the methane oxidation (R.3).

$$CH_4 + H_2O \leftrightarrow CO + 3H_2 \quad \text{R.1}$$

$$CO + H_2O \leftrightarrow CO_2 + H_2 \quad \text{R.2}$$

$$CH_4 + 2O_2 \rightarrow CO_2 + 2H_2O \quad \text{R.3}$$

Membranes in the reactor are double-skin Pd/Ag thin-layer cylindrical membranes. Since these membranes have a very high perm-selectivity (about 25.000 is the ratio between the moles of hydrogen and nitrogen permeated in pure gas tests at 500 °C [9]), it is here assumed that only hydrogen crosses the membrane. Therefore, the inner side of the membrane is a cylindrical space filled with pure hydrogen under vacuum conditions. Catalyst is a Rh-based fluidizable catalyst on an alumina support. A sketch of the structure of the FBMR is reported at the left side of Fig. 2. Parameters for permeation equations and for the kinetic model can be also found in Ongis et al. [30].

The membrane reactor model has been validated against experimental results obtained by Nooijer et al. for biogas reforming in a lab-scale fluidized bed membrane reactor [31]. A Rh-based fluidizable catalyst was used in a 4.27 cm diameter vessel, with and without a Pd-based membrane of 14.35 cm length and 14.26 mm diameter. Experiments used for the model validation are performed at a reactor temperature of 480 °C, a retentate pressure of 3 bar and a permeate-side pressure of 0.1 bar. A feed of 3.6 NL/min was fed to the reactor (0.00268 mol/s), with a content of 10% of methane, 30% of steam and a variable CO_2 content in various experiments (from 0 to 9%). The complement to 1 is always made by N_2 fraction. To validate the model against these results, film layer model has been used to include concentration polarization losses, as the polarization mass transfer value for the single-membrane case has been experimentally derived by De Nooijer [32]. Hydrogen flux $\dot{J}_{H_2}$ follows equation (1), where the subscript *bulk* refers to variable value in the retentate bulk while subscript *m* is the value by the membrane surface. *Pe* is the membrane permeance, that in experimental condition results 2.266 $\frac{kmol}{h \bullet m^2 \bullet bar^{0.5}}$, and $n = 0.5$.

$$\dot{J}_{H_2} = k_m \cdot C \cdot \ln\left(\frac{1 - x_{H_2,m}}{1 - x_{H_2,bulk}}\right) = Pe \cdot \left(p^n_{H_2,bulk} - p^n_{H_2,perm}\right) \quad (1)$$

The mass transfer coefficient k_m is assumed equal to 79.2 m/h, consistently with experimental evaluations on the single-membrane test [32]. Average concentration C is calculated with ideal gas law at retentate temperature and pressure ($C = \frac{n}{V} = \frac{p}{R \bullet T}$). The comparison between model predictions and experiments at different compositions is reported in Fig. 1. The model shows good agreement with experimental values.

Due to the deep connection between the operating and geometrical parameters of the reactor, in Ongis et al. [30] the reactor model has been used to investigate the effect of relevant parameters (pressure and temperature inside the reactor, vacuum-side pressure inside the membranes, steam-carbon-ratio, number, length and pitch of the membranes, feed flow rate, fluidization velocity) on reactor performance. Performance of the FBMR is expressed in terms of Hydrogen Recovery Factor (HRF) and pure hydrogen production, which are the kilograms of hydrogen separated through the membranes per unit time $\dot{m}_{H_{2,perm}}$. HRF is defined et al. as the ratio of pure hydrogen separated over the maximum theoretical amount of hydrogen that can be separated [26], as in equation (2), if all methane available for reforming reacts and all hydrogen produced is separated. This means, beyond the part of methane which undergoes to oxidation, that for each mole of methane, 4 mol of hydrogen are produced and then separated.

$$HRF = \frac{\dot{n}_{H_{2,perm}}}{4 \bullet \left(\dot{n}_{CH_{4,in}} - \dot{n}_{CH_{4,ox}}\right)} \quad (2)$$

Each working condition of the reactor (meaning that the value of all above mentioned parameters have been fixed) is represented by a point

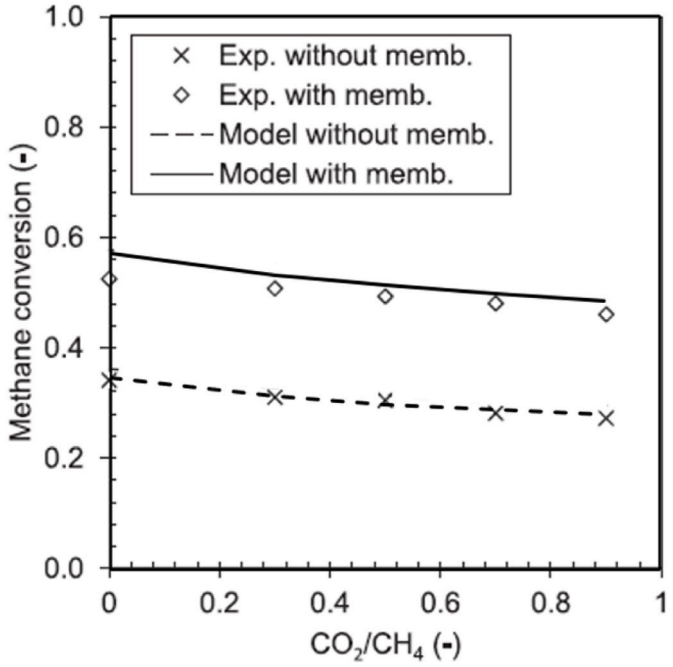

Fig. 1. Membrane reactor model validation against experimental results obtained by De Nooijer et al. [31]. Reactor is operated at 480 °C, 3 bar, with permeate pressure at 0.1 bar. Total flow is 3.6 NL/min. methane content is always 10% molar, and steam 30% molar. CO_2 is variated in different proportions with methane, and the rest is nitrogen.

in the $HRF - \dot{m}_{H_{2,perm}}$ plane, called performance chart. These charts allow to easily understand how the effect of a variation in operating condition influences the hydrogen production and the recovery factor. In Ongis et al. [30], almost all the relevant operating and geometrical parameters have been changed starting from a base-case. This allowed to understand how the reactor responds to any variation, to both support the design stage and the off-design operation. As an example, on the right side of Fig. 2, it is reproposed the chart from the same article, that shows a possible path to move from a starting design point A to a final desired point D by changing parameters such as the catalyst amount, the membranes length and the number of membranes.

Compared to the results in literature, in this work the performance charts are generalized to better understand what they represent and how can they support the reactor and process design stages. The analyses at reactor level, and their representation on the generalized performance charts, are described in section3.

2.2. System model: layout, assumptions and KPIs

The HRF provides an efficiency parameter for the membrane reactor; It does not, however, give information on the overall performance of the system in which the reactor is integrated. To properly optimize the overall system, information of auxiliaries' consumptions, such as vacuum pump and compressors, are necessary. In the same way, a thermal integration analysis is required using the heat released from retentate combustion and from permeate cooling, thus avoiding additional feedstock consumptions.

A process-level analysis is included in this work. Pure hydrogen production has been set to 100 kg/day, with a delivery pressure of 20 bar, consistently with the values set for a small-scale reference system without MR obtained by Di Marcoberardino et al. [5], to allow a comparison. The model of the system has been realized in Aspen Plus®, a well-recognized software for process simulations, which has available several packages for the simulation of the system components and a detailed calculation of the fluid properties. Peng-Robinson equation of state has been selected for the evaluation of thermodynamic properties of all substances. The FBMR model, developed in ACM, has been exported into process model as customized block.

Biogas flow rate is a variable which can be freely changed, while steam and air flow rates change accordingly to BG amount, the former in order to set a fixed Steam-Carbon-Ratio (SCR, the ratio between molar flow of steam over molar flow of methane) at the beginning of the membrane region (5 cm from the distributor plate of the reactor), and the latter to maintain autothermal behaviour of the reactor, considering that heat released from methane combustion have to balance the heat required by reforming reaction at the desired temperature. BG and air compositions are the same defined in Table 1. BG composition is representative of a typical anaerobic digestion plant, and is consistent to what had been used in Di Marcoberardino et al. [5]. Biogas humidity represents the saturated condition at 25 °C and 1 bar. Its Lower Heating Value (LHV) results 17.8 MJ/kg.

The proposed Hydrogen Production System (H2PS) layout is shown in Fig. 3. Biogas ① and air are compressed in different intercooled compressors and then mixed and heated - cooling down the exhaust gases - up to maximum temperature of 300 °C, to avoid methane

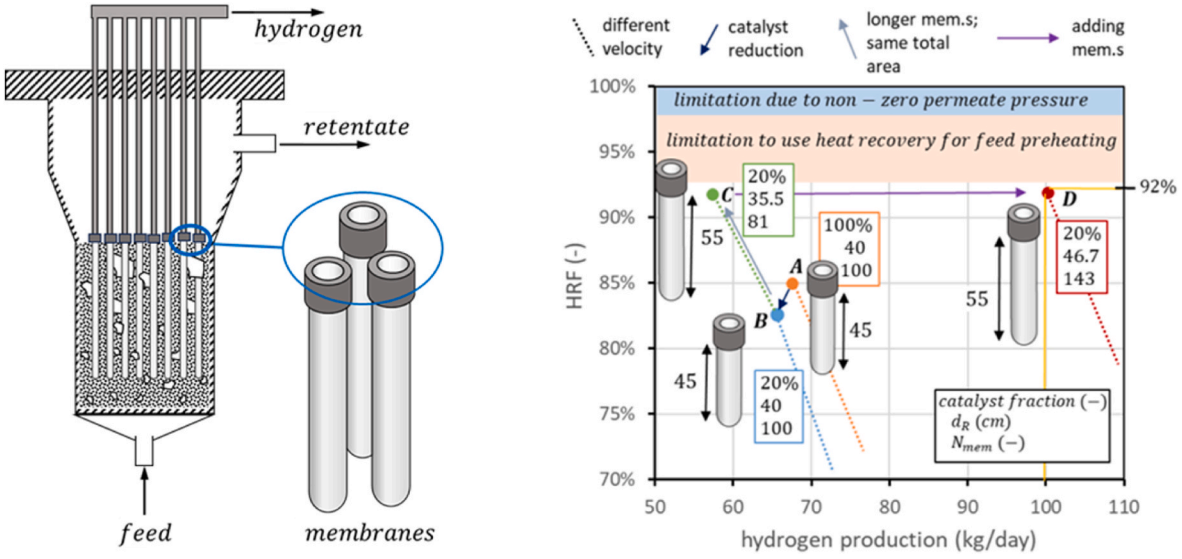

Fig. 2. On the left, FBMR layout. On the right, usage of performance charts to support reactor design. Both reproduced from Ref. [30].

Table 1
Biogas and air compositions.

Species	Biogas (%mol)	Air (%mol)
CH_4	58.1	0
CO_2	33.9	0
N_2	3.8	79
O_2	1.1	21
H_2O	3.1	0

oxidation occurring before the reactor. Water is fed into the pump and heated up through different heat exchangers (economizers ECO and ECO2, evaporator EVA and superheater SH). Biogas-air mixture ② is then mixed with steam, which was previously heated up to 700 °C, to guarantee in all cases a feed stream ③ temperature between 400 °C and 500 °C at the reactor inlet. Steam is produced with the thermal power supplied by the retentate and permeate cooling. In particular, the retentate ④ is oxidized into a catalytic burner, with an air addition to end up with an O_2 content in the combustion gases of 5% (dry molar basis). The permeate ⑥ leaves the reactor in sub atmospheric pressure and it goes through heat exchanger ECO, then it is cooled, pumped at atmospheric conditions in a vacuum pump and finally compressed at the delivery pressure in hydrogen compressor. The retentate, after going through the heat exchangers, is cooled to avoid the emission of hot flue gas and to recover part of steam in form of condensed water. The remaining flue gases represent the exhausts ⑤.

In terms of Key Performance Indicators (KPIs), the efficiency parameter for the overall H2PS has been defined in terms of primary energy [25] and is reported in equation (3).

$$\eta_{H2PS} = \frac{\dot{m}_{H_2,perm} \bullet LHV_{H_2}}{\dot{m}_{BG,in} \bullet LHV_{BG} + \frac{\dot{W}_{el}}{\eta_{el,ref}}} \tag{3}$$

where the hydrogen LHV is equal to 120 MJ/kg, $\dot{W}_{el}$ is the electric power of all auxiliaries, in MW, and $\eta_{el,ref}$ is the average electric efficiency of the power generating park. The mass flow of hydrogen $\dot{m}_{H_2,perm}$ refers to mass flow on the permeate stream ⑥ in kg/s. $\dot{m}_{BG,in}$ is the mass flow rate of biogas ① fed to the system, in kg/s.

The main assumptions for the parameters of the H2PS are listed in Table 2, and are mainly taken from Ref. [25], with the following two changes: (i) it has been added an electric consumption associated to the heat rejection performed via air coolers, equal to 1.5% of the discharged thermal power; (ii) the global heat transfer coefficients of the heat exchangers have been reduced to 40 $W/(m^2 \bullet K)$ for gas-gas heat exchangers and to 50 $W/(m^2 \bullet K)$ for gas-liquid heat exchangers and for the evaporator, compared to the values of 60 and 70 previously used, to be more conservative due to sometimes low pressures and sometimes low flow rates involved.

Moreover, it is assumed that the system is operated with the following constraints: (i) BG-air mixture is heated up to 300 °C, to avoid methane decomposition and methane oxidation to take place outside the reactor; (ii) minimum ΔT in the heat exchangers is always greater than 25 °C, (iii) temperature after the burner (hottest point) should be limited to 1000 °C to avoid excessive thermal stress on piping materials.

2.3. Economic analysis: methodology and assumptions

The economics is assessed using the Levelized Cost Of Hydrogen

Table 2
System parameters assumptions.

Parameter	Value	Units
Hydrogen production	100	kg/day
Hydrogen delivery pressure	20	bar
Ambient temperature	15	°C
Controller consumption (% of total auxiliary consumption)	10	%
Electric consumption in air coolers (% of thermal power)	1.5	%
Average electric efficiency of the power generating park	45	%
Water pump hydraulic/mechanical efficiency	0.7/0.9	–
Compressors isentropic/mechanical efficiency	0.7/0.85	–
Vacuum pump isentropic/mechanical efficiency	0.7/0.85	–
Minimum ΔT in heat exchangers	25	°C
ΔT subcooling in economizer	8	°C
Heat transfer coefficient gas/gas	40	$W/(m^2 \bullet K)$
Heat transfer coefficient gas/liquid (or two phase)	50	$W/(m^2 \bullet K)$

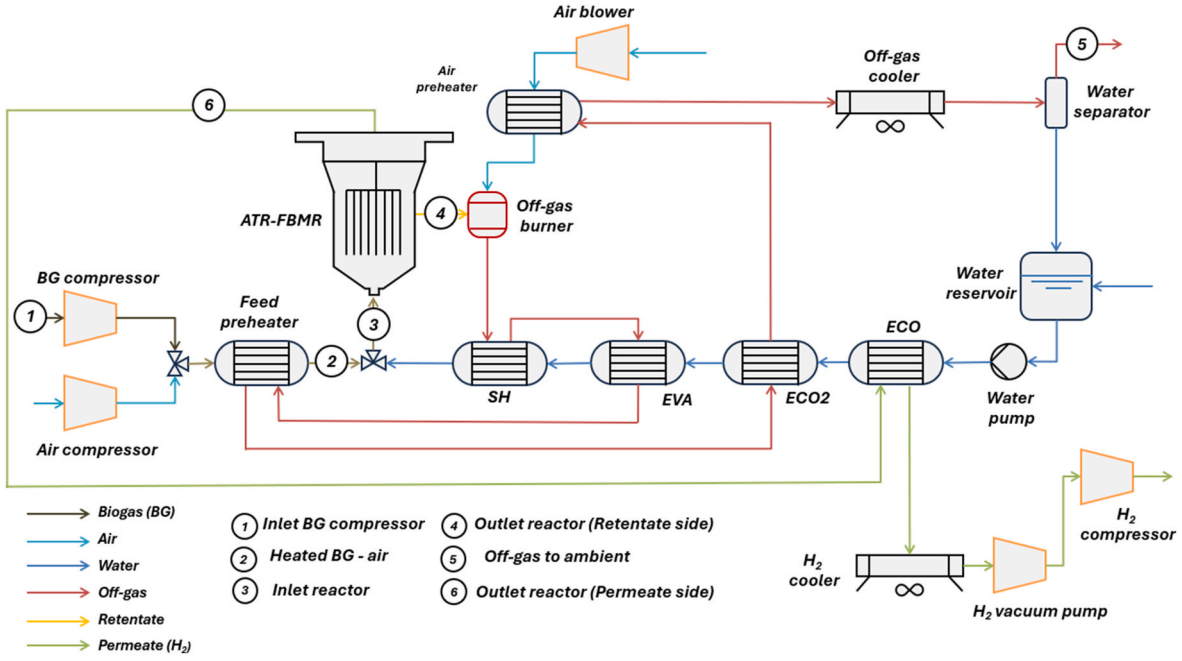

Fig. 3. H2PS layout including the FBMR for ATR. The layout is designed to maximize heat recovery from permeate and retentate stream and to be flexibly operated in all investigated conditions.

(LCOH), calculated according to the following equation [25,26,33]:

$$LCOH = \frac{TPC \bullet CCF + C_{O\&M_{fix}} + C_{O\&M_{var}} \bullet h_{eq}}{\dot{m}_{H_2,perm} \bullet 3600 \bullet h_{eq}} \quad (4)$$

where TPC is the Total Plant Cost, CCF the Capital Charge Factor, CO&M the Operation and Maintenance (O&M) costs, both fixed and variables, and h_{eq} the annual operating hours. TPC is calculated, starting from components' total cost (also known as Total Equipment Cost, TEC), by adding installation costs (TIC), indirect costs (IC) and owner's and contingencies cost (C&OC), all evaluated as a percentage additional cost [33].

$$TPC = \left(\sum_i C_{i,2019}\right) \bullet (1 + \%_{TIC}) \bullet (1 + \%_{IC}) \bullet (1 + \%_{C\&OC}) \quad (5)$$

Assumptions for the parameters used in economic KPIs are reported in Table 3, consistently with the values obtained in Di Marcoberardino et al. [34] for a similar plant.

Regarding the components cost, reactor vessel cost is calculated considering the cost for the raw material and a factor of 7 for the flanges, fittings and welding. Reactor is considered as a pressure vessel: the thickness of the reactor wall (t_R, equation (7)) is sized depending on the operating pressure (p_R), the internal radius ($\frac{d_R}{2}$), the weld joint efficiency (E, assumed 0.85) and the admissible tension S. S is calculated in equation (6), based on the Ultimate Tensile Strength (UTS) and the yield strength (σ_y) of the reactor material (T316 Stainless Steel), assumed respectively 110 MPa and 90 MPa. Starting from the thickness, the total amount of material is calculated considering a cylindrical shape of 1 m length. Formulas and methodology are taken from American Society of Mechanical Engineers (ASME) standard (BPVS-VIII-1-2021) [35]. The reactor is in all cases sized for a pressure of 6 bars above the operating pressure, for safety reasons.

$$S = \min\left(\frac{UTS}{3.5}, \frac{\sigma_y}{1.5}\right) \quad (6)$$

$$t_R = \frac{p_R \bullet \frac{d_R}{2}}{(S \bullet E - 0.6 \bullet p_R)} \quad (7)$$

Membranes cost is accounted both as plant costs and as annual fixed operating costs, the former due to their initial installation and the latter due to necessary substitutions along the plant lifetime, due to the necessity of their replacement, assumed every five years. Catalyst cost is calculated starting from the material costs, assuming an average cost of 26.9 €/kg for ZrO_2, taken from a commercial producer [36], and a cost of 137,205.0 €/kg for pure Rhodium (average value of 2019) [37]. Zirconia oxide represents both the support of the catalytic pellet (98.4% of the mass of the particle) and the filler particles (100% ZrO_2). Assumptions for the costs related to the membrane reactor elements are listed in Table 4.

Regarding the other components' costs, $C_{k,2023}$ are calculated from literature, using a reference size $S_{k,0}$ and cost $C_{k,0}$ and then scaled up with equation (8), taken from Di Marcoberardino et al. [25], which also reports the costs from the reference year y to 2023 by using the Chemical Engineering Plant Cost Index (CEPCI).

Table 3
Parameters used for TPC and LCOH calculation [25].

Parameter	Value	Units
$\%_{TIC}$	0.65	–
$\%_{IC}$	0.14	–
$\%_{C\&OC}$	0.15	–
CCF	0.16	–
h_{eq}	7500	h/y

Table 4
Cost assumptions for the FBMR elements.

Parameter	Value	Units
Stainless steel 316L raw material	3.5	€/kg
Vessel cost to raw material cost ratio	7	–
Catalytic particles (lifetime 5 years)	2221.75	€/kg
Filler particles (lifetime 5 years)	26.9	€/kg
Membranes (lifetime 5 years) [38]	5.5	k€/m^2

$$C_{k,2023} = \left(C_{k,0} \bullet \left(\frac{S_k}{S_{k,0}}\right)^f\right)_y \bullet \frac{CEPCI_{2023}}{CEPCI_y} \quad (8)$$

Reference costs for H2PS components are reported in Table 5. They are mainly taken from Ref. [5], but some costs that have been introduced or refined, such as addition of air coolers cost and refinements of costs of hydrogen compressor and hydrogen vacuum pump.

Beyond components' costs, LCOH calculation includes O&M variable (dependent on the operating hours) and fixed costs. They include feedstock, electric energy, maintenance, insurance, and labour cost. Membranes and catalyst replacements costs are calculated from their specific costs (listed in Table 4) divided by their assumed lifetimes (5 years in both cases). Assumptions for O&M costs are reported in Table 6, as well as the CEPCI index.

3. Membrane reactor analysis

3.1. Generalized performance charts

A performance chart is here defined as a chart with the hydrogen production $\dot{m}_{H_2,perm}$ in the x-axis and the HRF in the y-axis. When a reactor geometry is chosen (vessel diameter, number of membranes immersed, length of the membranes – and then of the reactor) and all operative conditions are set (reactor temperature – assumed uniform – and pressure, pressure inside the membranes, temperature of the feed, amount of catalyst, feed flow rate and composition), the hydrogen production and the HRF can be computed by the reactor model and the corresponding point displayed on the performance chart. The opposite cannot be stated: a same specific point can be reached for different combinations of the reactor geometry and of the operative conditions.

In [30], to investigate the influence of each parameter, they were all fixed in a base-case except for the biogas flow rate (and consequently the fluidization velocity regime, related to the ratio $/u_{mf}$) and one parameter at each time, which was the investigated variable. In this way, the authors ended up, for each variable, with a family of performance lines. Each line could be obtained specifying the value of the variable investigated, and it is possible to select each point on the line by changing the

Table 5
Cost assumptions for plant components. If not specified otherwise, from Di Marcoberardino et al. [5].

Components	Scaling parameter	$S_{k,0}$	$C_{k,0}$ (k€)	f	Year cost	$CEPCI_y$
Heat exchanger	Exchange area [m^2]	2	15.5	0.59	2007	525.4
Air cooler - heat exchanger [39]	Exchange area [m^2]	200	139.3	0.89	2001	394.3
Biogas compressor	Power [kW]	5	3.3	0.82	2006	499.6
Air compressor	Power [MW]	0.68	3.42	0.67	2009	521.9
Water pump	Water flowrate [l$_{H2O}$/h]	90	1.2	0.7	2011	585.7
H_2 compressor [23]	Electric power [kW]	10	27.5	0.82	2006	499.5
Vacuum pump [40]	Electric power [kW]	4.09	25	0.44	2017	567.5
Burner	–	–	5	–	2013	567.3

Table 6
O&M costs and CEPCI. If not specified, taken from Di Marcoberardino et al. [5] or calculated.

Parameter	Type	Value	Units
Electric energy	Variable	0.12	€/kWh
Biogas [3]	Variable	27.12	c€/Nm^3
Deionisation resin	Fixed	447.07	€/y
Maintenance	Fixed	2	% Of TPC
Insurance	Fixed	2.5	% Of TPC
Labour cost	Fixed	30	k€/y
Catalyst replacement	Fixed	444.35	€/(y•kg)
Filler replacement	Fixed	5.38	€/(y•kg)
Membranes replacement	Fixed	1.1	€/(y•m^2)
$CEPCI_{2023}$ average [41]	–	790	–

biogas flow rate, and then the fluidization velocity. That analysis, although useful to understand the effect of each parameter, had the drawbacks to be extremely specific for a base-case scenario in which most of the variables are fixed.

A further step is presented in this work about the generalization of the performance charts. As indeed resulted in Ongis et al. [30], variations in membranes length or in membranes pitch (then reactor diameter), at constant total membrane area, led to the same shift of the working point to what can be obtained working at different velocities. A numerical example is also reported in Supplementary Materials, where, starting from a working point where 80 kg/day of hydrogen are separated with HRF = 66%, another working point, with 98 kg/day of production and HRF = 38.4%, is reached increasing biogas flow rate in three different routes: increasing also gas velocity (at fixed geometry), increasing pitch (at fixed velocity and membrane length) and decreasing membrane length (at same velocity and pitch). In other words, a performance line represents all the points obtained, at fixed total membrane area, by changing the feed flow rate and, accordingly, one or more among: (i) fluidization velocity, (ii) membranes' pitch and (iii) membranes' length.

Another step towards generalization of the problem is to understand what happens when the total membrane area is changed. An example of performance lines at different total membrane area is reported in Fig. 4a. In Ongis et al. [30], it had already been observed that, fixing the HRF, an increase in the number of membranes enhances proportionally the hydrogen production. It can be therefore stated that performance lines are a family of lines in which, set the HRF, the hydrogen production is proportional to the membrane area. This allows us to draw a generalized performance line, in a generalized performance charts, where y-axis is still HRF but x-axis is the specific hydrogen production per unit of total membrane area $\dot{m}_{H_2,perm}/A_{mem}$. Generalized performance line, corresponding to the points on Fig. 4a, is reported on Fig. 4b.

The results obtained in this generalization can be summarized as follows: once are fixed (i) reactor temperature T_R and (ii) pressure p_R, (iii) vacuum-side pressure p_p, (iv) SCR, (v) feed temperature T_{feed} and (vi) the Weight Hourly Space Velocity (WHSV - that is the ratio between methane flow rate (kg/h) and the catalyst mass packed (kg)), all the possible working points of the FBMR for biogas ATR lie on a single line in the generalized performance chart, with HRF in y-axis and the specific hydrogen production per unit of membrane area, $\dot{m}_{H_2,perm}/A_{mem}$, in x-axis. It is possible to move along this line, called generalized performance line, by changing $\dot{n}_{BG}/A_{mem}$ ratio. Accordingly, one (or more) of the following parameters should change: membrane length L_m (maintaining the same total membrane area, so correspondingly changing the number of membranes, then reactor diameter), membranes pitch d (then reactor diameter) or fluidization velocity, represented by the ratio between superficial velocity and minimum fluidization velocity u/u_{mf}. Once fixed two of these variables, the third one is uniquely determined.

This generalization simplifies the Techno-Economic Analysis (TEA), reducing the number of parameters that should be analysed and then saving complexity and computational time. Instead of running several simulations for different values of L_m, d (therefore u/u_{mf}) and the number of membranes, only the total membrane area is a relevant parameter that will be included in the TEA. From a technical standpoint, the specific combination of fluidization velocity, pitch, and membrane length used to reach the working point is not relevant, as the system treats the reactor as a black box with the same input-output relationship TEA will then assess only the optimal conditions in terms of total membrane area.

The best reactor design with a fixed total membrane area can be derived from technical constraints and general economic considerations on its costs; this is done in the next section.

3.2. Reactor cost minimization

Although, from an external perspective, the distribution of membrane area within the reactor may appear irrelevant—since the reactor functions as a black box with consistent hydrogen production and retentate composition—certain combinations of L_m, d and u/u_{mf} preferable from the reactor's internal perspective.

In real operations, the constraints in this sense are typically technical

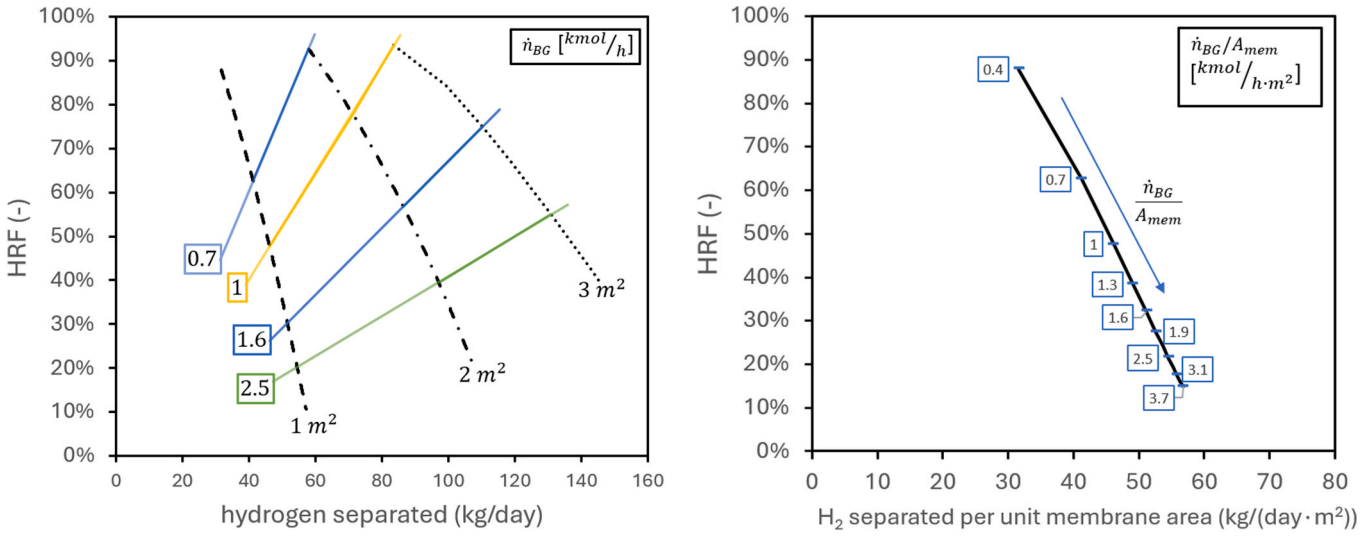

Fig. 4. (a) performance lines at different values of the membrane area in a performance chart. Values in squares represents the biogas flow rate (kmol/h). (b) The resulting generalized performance line on the generalized performance chart. Values in squares are the specific biogas flow rates per unit membrane area. (T_R = 500 °C, p_R = 12 bar, p_p = 0.1 bar, SCR = 3, T_{feed} = 400 °C, WHSV = 0.5 h^{-1}).

and they are related to the technology development (as in the case of the membrane length, since it is hard to produce very long membranes or to seal in series a lot of short membranes without leakages) or sometimes related to the physics of the problem (as in the case of the membrane pitch, that should not go under 3.4 cm to avoid a steep increase of the concentration polarization (CP) losses [42], or the velocity that cannot be too high to avoid the risk of elutriation). Beyond the technical problems, it is however possible to state some general conclusions from a simple modelling point of view.

A first straightforward consideration is about the membranes' pitch. A higher pitch means a larger reactor, and the vessel thickness t_R linearly increases with reactor diameter d_R. This leads to more material to build up the reactor and then a higher reactor cost. Moreover, a higher distance among the membranes increases the risk of gas bypass, meaning that hydrogen reaches the top of the reactor without running into the membrane surface, even if this effect is not accounted for in the model. It then can be a good practice to keep the pitch as small as possible, being careful not going too close to avoid a steep increase of the CP losses. This minimum distance should be in general verified experimentally, but as mentioned for this process and membranes is about 2 cm side-to-side of two adjacent membranes (3.4 cm pitch).

The other consideration is about the combination of membranes' length and fluidization velocity. Given a set total membrane area, the longer the membranes, the lower is the number of membranes that should be fitted into the reactor. Once the pitch is fixed, if the membrane length is also set, the ratio u/u_{mf} (which is a function of the axial coordinate) is consequently determined, and the velocity increases if the membrane length increase. The reason for this trend lies in the fact that when more membranes are present into the reactor, since a minimum pitch should be guaranteed, the cross section of the reactor available for the gas to flow (that is, reactor cross section minus the cross section of all the membranes) increases, and consequently the gas velocity decreases.

To summarize these considerations with an example, a single working point has been obtained for different combinations of L_m, d and u/u_{mf}. Results are reported for this specific point, but the results can be generalized. HRF is 91.7% with a hydrogen production of 67.6 kg/day. The total membrane area is 2 m^2 and BG flow rate 0.749 kmol/h. In Fig. 5, different combinations of L_m, d and minimum u/u_{mf}, are reported. It can be noted that the velocity increases as membrane length increases and, for a given length, it decreases if the pitch grows, since the cross section of the reactor increases. The cost of the reactor is compared in the analysed cases, in terms of the cost of the metallic vessel and of the filler material. Membrane cost, being related only to total area, and catalyst cost, related to WHSV, are indeed considered the same for all the cases. The filler material depends on the reactor volume and the fluidization conditions. The effect of the pitch is quite straightforward: if it increases then the reactor diameter increases, and accordingly the vessel and filler costs increase due to a higher reactor diameter and then volume. Smaller pitches are therefore preferred from an economic point of view. Fixed the pitch, the costs comparison shows that it is convenient to use longer membranes and, accordingly, faster fluidization conditions.

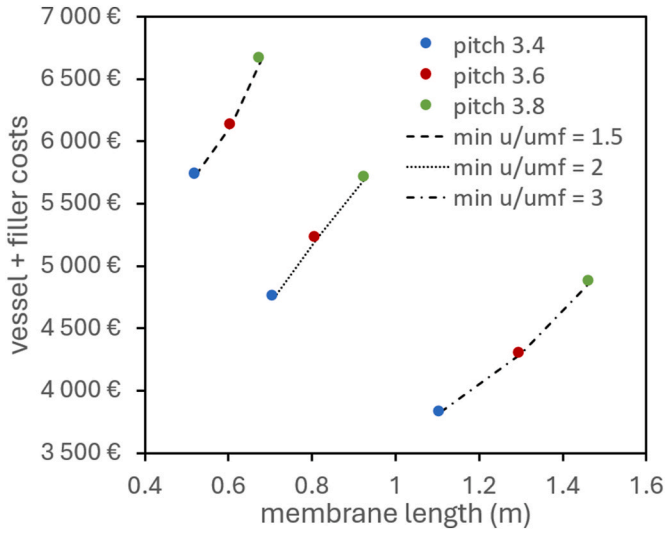

Fig. 5. The same working point on the performance chart obtained for different combinations of membranes' length, pitch and fluidization velocity. Results are obtained at $\boldsymbol{T_R}$ = 500 °C, $\boldsymbol{p_R}$ = 12 bar, $\boldsymbol{p_p}$ = 0.1 bar, SCR = 3, $\boldsymbol{T_{feed}}$ = 400 °C, WHSV = 0.15 $\mathbf{h^{-1}}$. Biogas flow rate is 0.749 kmol/h. The working point obtained is HRF = 91.7% and $\boldsymbol{\dot{m}_{H_2\,perm}}$ = **67.6 kg/day**.

It is therefore possible to conclude that, in reactor design, it is convenient to maintain a small pitch, limiting the value over a minimum to avoid strong concentration polarization, and to design the reactor with long membranes and high velocities, up to the technological limits of membrane production and the velocities that avoid the elutriation phenomena.

3.3. Use of performance charts in techno-economic analysis

In this section the performance charts are extended to the overall system level. The question that arises from the system TEA is: which working point should be chosen to obtain a desired hydrogen production at minimum cost? Once $\dot{m}_{H_2,perm}$ is set, it is possible to move along the performance line by changing the membrane area and to select any of the working points. This is illustrated on the generalized performance chart at the left side of Fig. 6. At the centre, the same is depicted on the performance chart (so hydrogen production on x-axis is no more specific on membrane area). To answer the question, the TEA shows that there is a trade off between the feedstock cost (which increases as HRF decreases) and the membranes cost (which increases as the membrane area increases). As shown at the right side of Fig. 6, TEA results can be expressed in terms of LCOH over the total membrane area: it is expected to be found a membrane area that minimizes the LCOH, which represents the optimal working point.

With this procedure, it is possible to find the optimum working point on a single generalized performance line. However, such a line depends on feed and reactor temperatures, reactor pressure and pressure inside the membranes, SCR and the WHSV. Therefore, an optimum working point must be selected for each set of these parameters. In other words, whenever one or more of these variables change, the performance lines change shape and the analysis of Fig. 6 should be repeated. The optimum working points of the different conditions are then compared, to find an overall optimum. The procedure is displayed in Fig. 7 using as an example the effect of two different pressures. It will be further clarified in the next section, where the actual TEA is performed.

4. System techno-economic analysis

In all analyses, the H2PS is designed such that 100 kg/day of pure hydrogen are produced. Among the operating variables, T_R, p_p and SCR are fixed, while the temperature of the feed T_{feed} is the result of the heat integration of the system. The feed is preheated from the hot retentate, as displayed in Fig. 2, and then its value is not fixed but depends on the specific case study. It is however guaranteed that, in all cases, its value is bounded between 400 °C and reactor temperature T_R, to facilitate the isothermal behaviour of the reactor avoiding strong thermal gradients inside. Regarding the catalyst amount, preliminary calculations showed that a value of WHSV = 0.5 h^{-1} guarantees in all cases to be close to the near-equilibrium condition (meaning that an additional amount of catalyst does not changes appreciably the performance of the reactor). The effect of operating pressure is investigated between 9 and 18 bar.

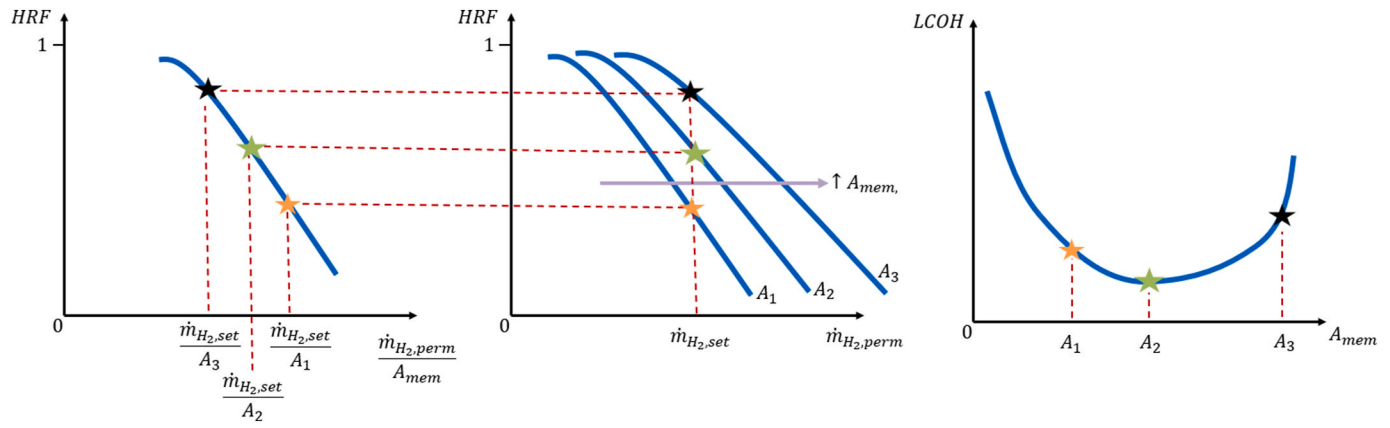

Fig. 6. Visualization of the procedure to select the best working point from the economic point of view. On the left, the possible working points on the generalized performance chart. At the centre, the same points visualized on the performance chart. On the right, example of the trend of LCOH obtained for the different working points. In this case, membrane area A_2 corresponds to the best condition, as the LCOH is minimum.

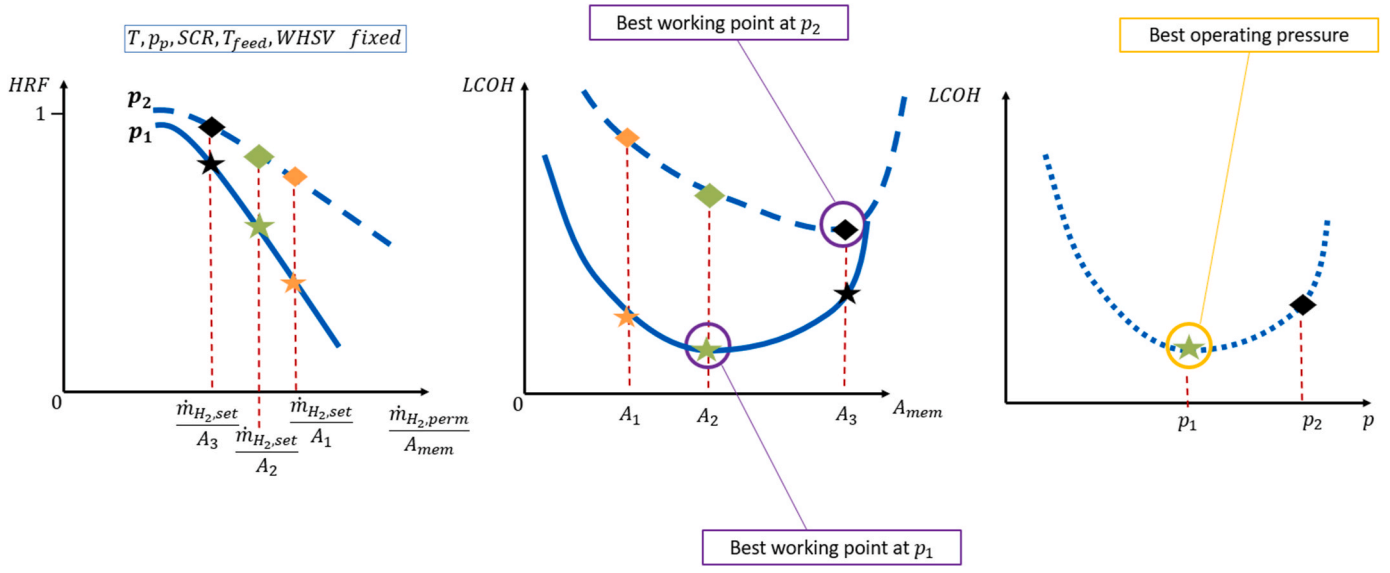

Fig. 7. Procedure of the TEA for the system optimization. For each set of the operating variables, a working point is selected as the one which values of membrane area and HRF minimize the LCOH.

4.1. System design

Design operating conditions have been defined considering state-of-the-art values for membrane reactors and are reported in Table 7.

The purpose of the technical analysis is to evaluate the trade-off between total membrane area and HRF at different pressures, to identify the working point which minimizes LCOH, as previously presented in Fig. 6. In general, more membranes in the reactor lead to a higher HRF, thus a higher system efficiency and lower biogas cost, as already reported in Ongis et al. [26]. Adding membranes increases the cost of the membranes itself and of the heat exchangers, since the temperature of the off-gas is lower and therefore higher exchangers' areas are required.

As an example, at 12 bar of pressure the results in terms of system efficiency and LCOH in the conditions identified in Table 7 are shown in Fig. 8. As expected, higher total membrane area improves HRF and then system efficiency, while reducing biogas costs that drives towards a lower LCOH. A minimum is found close to the limit of the thermal integration, meaning that above that membrane area the retentate LHV is too low to guarantee the thermal power input for steam generation. The steep rise in costs before that region is the sign that one heat exchanger had very low temperature driving force and therefore its area tended to diverge.

The minimum of LCOH is obtained using a membrane area of 2.87 m^2, that corresponds to a HRF of 83% and a system efficiency of 59.8%. Using commercial membranes (45 cm length), this correspond to 145 membranes. It is important to underline that LCOH values in Fig. 8, as well as values just reported on costs proportions, do not include the costs of the reactor vessel and the cost of the filler. This is because, as turned out from reactor analysis, TEA is done in terms of total membrane area,

Table 7
Parameters values of the base-case.

Parameter	Units	Design values
Reactor temperature, T_R	°C	500
Reactor pressure, p_R	bar	From 9 to 18 bar
Permeate pressure, p_p	bar	0.1
SCR	–	3
WHSV	h^{-1}	0.5
T_{feed}	°C	From 400 to T_R
Total membrane area A_{mem}	m^2	From 2.5 to 3 (125–150 membranes of 1.4 diameter and 45 cm length)

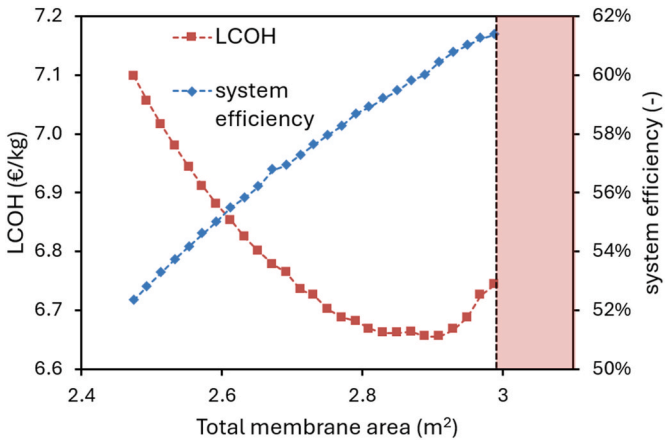

Fig. 8. Results of sensitivity analysis on membrane area in design case. The red region on the right indicates the membrane areas that cannot be used accordingly to the constraints on thermal integration. Pressure is 12 bar. (For interpretation of the references to colour in this figure legend, the reader is referred to the Web version of this article.)

but the vessel and filler costs change depending on how membranes are distributed. Using average values obtained in the simulations, it can be assumed 10 k€ for the vessel and 1.5 k€/y for the filler. This corresponds to an addition of +0.16 €/kg to the LCOH. Another +0.68 €/kg must be added in case also high-pressure hydrogen compressor is also considered.

Pressure variations have a trade-off effect on the MR behaviour: reforming reaction is favoured at lower pressures, and therefore equilibrium conversion of methane is higher; on the other hand, a lower pressure means a lower partial pressure of hydrogen, and then a lower driving force for permeation. Moreover, moving to the system level, lower pressure means lower power for BG and air compressors. Reactor pressure is then investigated in the range 9–18 bar. Fig. 9 summarizes the effect of operating pressure on HRF (reactor level, (a)), system efficiency (technical system level, (b)) and LCOH (economics, (c)). From the technical point of view, both reactor (HRF) and system performance seem to be affected such that a higher operating pressure means to reduce membrane area. HRF curves and η_{H2PS} translate to the left as pressure is increased. Therefore, the improvements in partial pressure of hydrogen and then in permeation driving force is higher than the partial pressure reduction due to lower hydrogen presence as its equilibrium conversion is reduced. This consideration is also useful to control the MR during its operation: if some membranes are removed in case of damages, a higher pressure could compensate allowing the same HRF and hydrogen production at lower total membrane area. Regarding LCOH, its trends over membrane area is reported in Fig. 9c. The trends obtained by the simulations show that there is a plateau in LCOH between 10 and 15 bar. At fixed membrane area, at higher pressures the HRF increases, and the system efficiency increases consistently. However, since at a certain point the boundary of thermal integration is reached and then performance cannot be improved anymore, the gain shift towards reaching the same efficiency with less membranes. In this sense, the minimum in LCOH stays about the same in absolute values: among 10 and 15 bar the minimum is always approximately 6.65 €/kg. While at

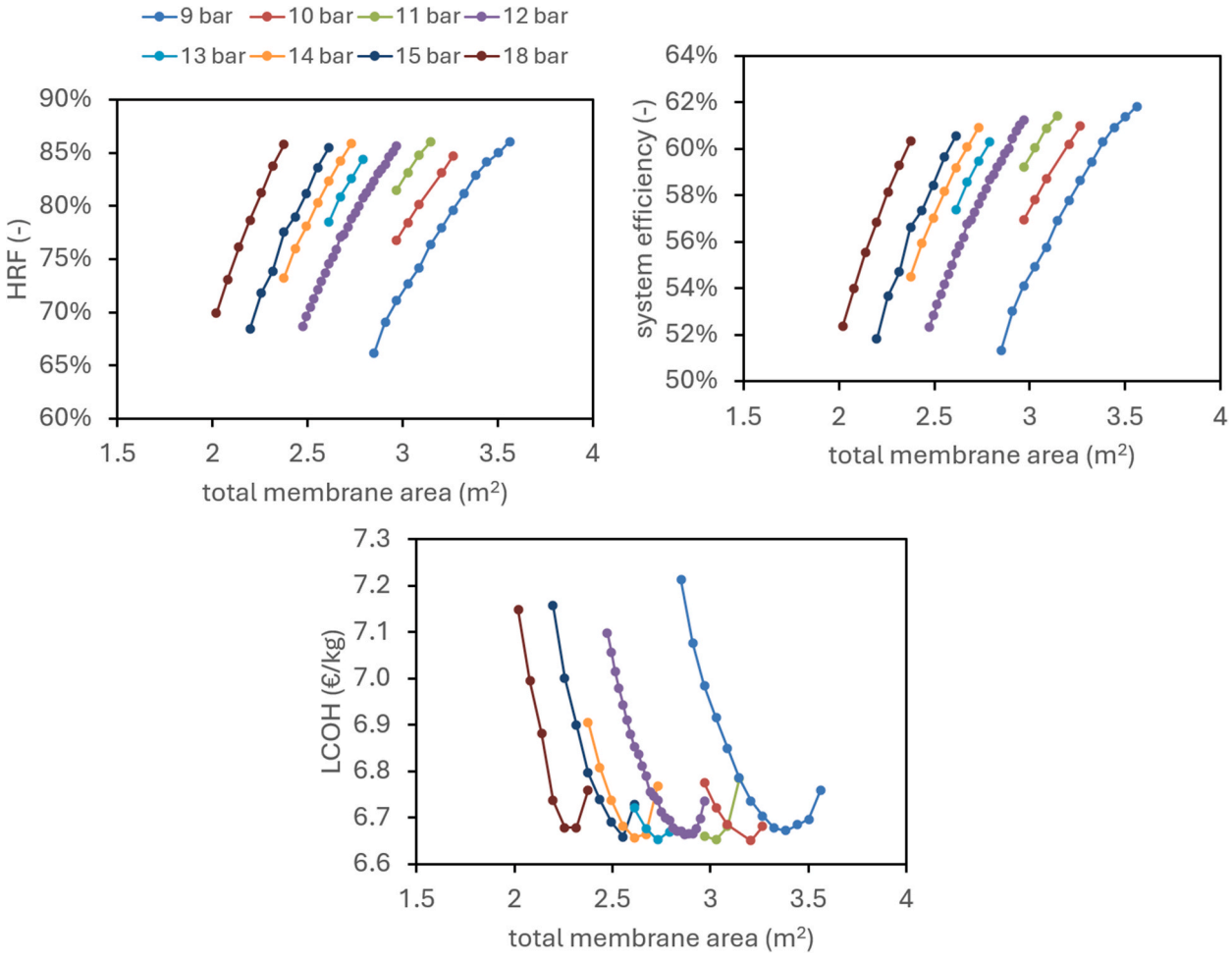

Fig. 9. Effect of operating pressure on reactor and system performance and costs. As dots, the points simulated.

both extremes, at 9 and 18 bar, the minimum LCOH slightly rises. The plateau between 10 and 15 bar is due to competitive effect of pressure variations on LCOH: higher pressures mean higher compression costs, including a bit higher energy cost. On the other hand, it allows to have a similar system efficiency with a lower membrane number. Costs seem to increase at both extremes (9 and 18 bar), due to a predominant effect of membrane cost and of compression cost (with a final LCOH of 6.68) respectively. However, deviations are very small and given the pressure trends, the selected pressure to detail the results is 12 bar, in the centre of the range.

4.2. Material and energy balances in design conditions

Design conditions are the ones presented in Table 7, with 12 bar of operating pressure and a membrane area of 2.87 m^2 (145 membranes), corresponding to the minimum LCOH in these conditions. For this case, stream results, technical results and economic results are hereby reported. Flow rates, temperatures, pressures and compositions of the streams are reported in Table 8, where the stream indexes are referred to Fig. 3.

To quantify electric consumptions and thermal management, together with system efficiency, in Fig. 10 are reported Sankey diagrams that represents the different energy duties involved. In Fig. 10a the reactor level: biogas LHV, which is due to its methane content, mostly (72%) undergoes to reforming reaction, while about 10% remains unconverted and 18.5% is burned to provide heat for the reforming reaction and to heat up the feed stream from 438 °C up to 500 °C. The hydrogen generated and then separated through the membranes has a LHV of 138.9 kW (about 82% of inlet biogas), while retentate stream has a LHV of about 24.6 kW, given by hydrogen not removed, methane unconverted and CO. The other source of energy of the system that appears in the denominator of system efficiency in equation (3) is the primary energy used to produce the electric input duty of the system. Most of this energy (55%) is lost in the conversion process to electricity, while electricity is mostly consumed by the vacuum pump and hydrogen compressor. Different electricity duties are reported in Fig. 10b. System efficiency is obtained by the ratio between hydrogen separated (138.9 kW) and the sum between biogas LHV (170.2 kW) and primary energy input (62.1 kW), and it results $\eta_{H2PS} = 59.8\%$. It is worth mentioning that this value is obtained by associating primary energy with the electricity. If electricity is considered as an input, so analyzing the efficiency more at the level of the plant, the efficiency would be 70.1%.

Regarding the economics, including vessel and filler costs, the LCOH goes from 6.65 €/kg to 6.81 €/kg, which represents the costs for the production of hydrogen at 20 bar. O&M costs influence the LCOH by about 70% and TPC for the remaining 30%. The latter resulted 404.3 k€ and is made by about 46% from the costs of the components and the other 54% by installation, indirect and contingencies costs, whose values are proportional to the costs of the components. The major contributions to the components cost (TEC), which resulted 186.9 k€, are given by the heat exchangers (38.7%), the membranes (8.4%) and the hydrogen pressure changers (vacuum pump and compressors, 40.5%). Regarding O&M, estimated at about 148 k€/y, the main contributions are the biogas cost (about 40.5%), the electricity cost (17%) and the labour cost (20%). In case a higher pressure is required, such as for hydrogen storage at 700 bar for transportation, the costs for an additional compressor should be added. Assuming a cost of 30 k€ for the compressor, and an estimated additional electric consumption of 8.22 kW, the LCOH reaches 7.49 €/kg. System efficiency drops to 55%. Therefore, costs reported in this article (6.65 €/kg) refers to a production at 20 bar without vessel and filler costs; to end up with a value including also filler and vessel, the additional LCOH is about +0.16 (6.81 €/kg). For the high-pressure (700 bar) hydrogen production case, LCOH should be further added by +0.68 €/kg (7.49 €/kg).

Technical results are consistent, although more conservative, with the ones previously obtained by Ongis et al. [26], where system efficiency resulted 62.7%, and with the ones obtained by Di Marcoberardino et al. [25], where resulted 66.1%. Economic results however differs, since LCOH resulted 4.39 €/kg in the article of Ongis et al. [26] and 4.1 €/kg in Di Marcoberardino et al. [25], considerably lower compared to this work. This is mainly due to the rise in the CEPCI index, compared to its value in 2020, and to the refinement of some components' costs. TPC share is now increased (in Ongis et al. [26] was only about 10% of the LCOH, in this work is 30%).

4.3. Comparison with benchmark

In Di Marcoberardino et al. [5], pure hydrogen production from biogas with a small-scale reforming plant have been studied (layout is reported inFig. 11a). Both autothermal and external-heated configurations were studied in a techno-economic assessment, considering different system pressures. Hydrogen was purified using a vacuum pressure swing adsorption unit. Biogas molar composition is the same used in this article, as well as the hydrogen production set to 100 kg/day at 20 bar. It is therefore possible to adapt the values of the article in literature to set a benchmark cost for the same hydrogen production. Best system efficiency reported in the article is for the steam reforming configuration (external-heated) at 12 bar, where a value of 51.7% was reached. This value dropped to 46% considering hydrogen production at 700 bar. From thermodynamic point of view, membrane reactor configuration has a relevant improvement in terms of system efficiency (59.8% vs 51.7% at 20 bar).

To obtain a consistent comparison, the economic analysis of the benchmark case has been reproduced, by updating all economic assumptions consistent with this article. In particular, the cost of biogas, as well as different correlations for H_2 compressor and vacuum pump, were updated together with the labour cost and the different heat transfer coefficients in heat exchangers, that leads to different areas. Lastly, CEPCI index used in the benchmark was the value of 2017 (562.1), while in this work has been updated to the higher value of 2022 (790). The new LCOH value for the benchmark resulted in 7.31 €/kg for hydrogen production at 20 bar, and 7.98 €/kg at 700 bar. These values can be compared with the MR-based values of 6.81 €/kg and 7.32 €/kg respectively. Relative cost reduction using MR-solution is about 8% on the final LCOH.

As it is clearly displayed in the bar diagrams in Fig. 11b, the difference in LCOH between MR and benchmark cases is due to their different biogas consumption. All other voices slightly differ, but it can be

Table 8
Thermodynamic conditions, compositions and flow rate of the main streams in the design conditions in the working point which minimizes LCOH.

Stream	Flow		T_R (°C)	p_R (bar)	Composition (% molar basis)						
	Molar (mol/s)	Mass (g/s)			CH_4	H_2	CO	CO_2	H_2O	O_2	N_2
1	0.37	9.57	15	1	58.10	0	0	33.90	3.10	1.10	3.80
2	0.72	19.80	300	12	29.48	0	0	17.20	1.57	10.90	40.84
3	1.12	26.94	438	12	19.01	0	0	11.09	36.53	7.03	26.34
4	0.85	25.78	500	12	2.43	3.12	1.05	36.21	22.47	0	34.72
5	1.19	38.11	40	1	0	0	0	28.29	6.30	4.63	60.78
6	0.57	1.16	500	0.1	0	100	0	0	0	0	0

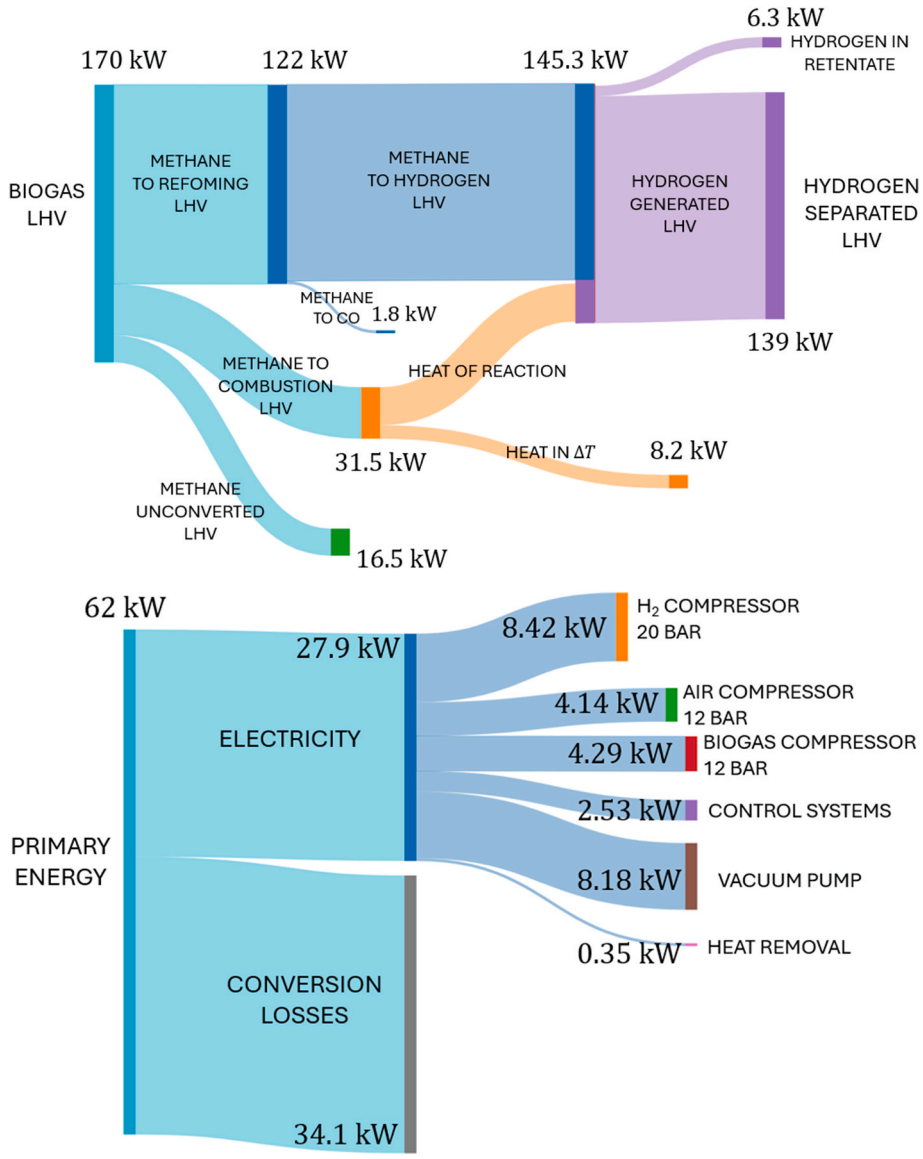

Fig. 10. Sankey diagrams for the membrane reactor (top) in LHV terms and for the electric energy duties of the system. Made with sankeymatic.com.

observed that, neglecting biogas costs, the LCOH of the two solutions were comparable. Different biogas consumption is therefore the main improvement of the MR solution, which is reflected in the higher system efficiency. The utilization of the biogas can be attributed to two factors: the conversion of methane (i.e. the ability to generate hydrogen) and a hydrogen recovery (i.e. the ability to separate hydrogen). In the design case, hydrogen recovery is 95.6% and methane to H_2 conversion (not including the share of methane combusted) is 86.8%, with a resulting HRF of 83%. In benchmark, methane conversion is the equilibrium value at 800 °C with SCR = 4, and results 87.5%, while only 57.1% of hydrogen is recovered in the PSA. The corresponding HRF results 49.9%. It can therefore be concluded that MR allows a substantial reduction of operating temperature (500 °C vs 800 °C) with a similar methane conversion, but its main advantage is due to membrane ability to separate more hydrogen, which is reflected in saving in biogas needs.

4.4. Sensitivity on economic analysis

The H2PS is a quite new solution for industrial applications, so economic evaluations still suffer from a relevant level of uncertainty. For this reason, a sensitivity analysis on the most important economic parameters has been performed.

Economic parameters investigated are the ones with major impact of the LCOH and with major uncertainty: the BG cost, membranes costs, electricity cost, labour cost and the pressure changers that process hydrogen. BG cost assumed in this work is an average value of BG production cost worldwide, which can locally differ from its price on the market. The standard cost considered was 0.2712 €/Nm^3 (44.26 €/MWh), while as market value is assumed 0.516 €/Nm^3 (84.2 €/MWh). About electric energy price, an average EU price for industrial applications is considered [43]. The annual electric consumption is calculated to be about 210 MWh/y. Considering the electricity price from 2018 to 2021 for industrial application and for the 20–500 MWh/y utilization range, an average electricity price of 18.93 c€/kWh has been taken as high value. Regarding membranes, there is both uncertainty on their market price, due to their still low commercialization, and regarding the necessary membrane area. Indeed, concentration polarization losses have been neglected in this analysis ($k_m \rightarrow +\infty$), due to their expected reduced entity in fluidized bed and the lack of a valid correlation [44], especially to estimate their value in fluidization. Given all these factors, a considerable cost addition (10 times) is assumed for the high-value case, ending up with 55 k€/m^2. A similar consideration is made for

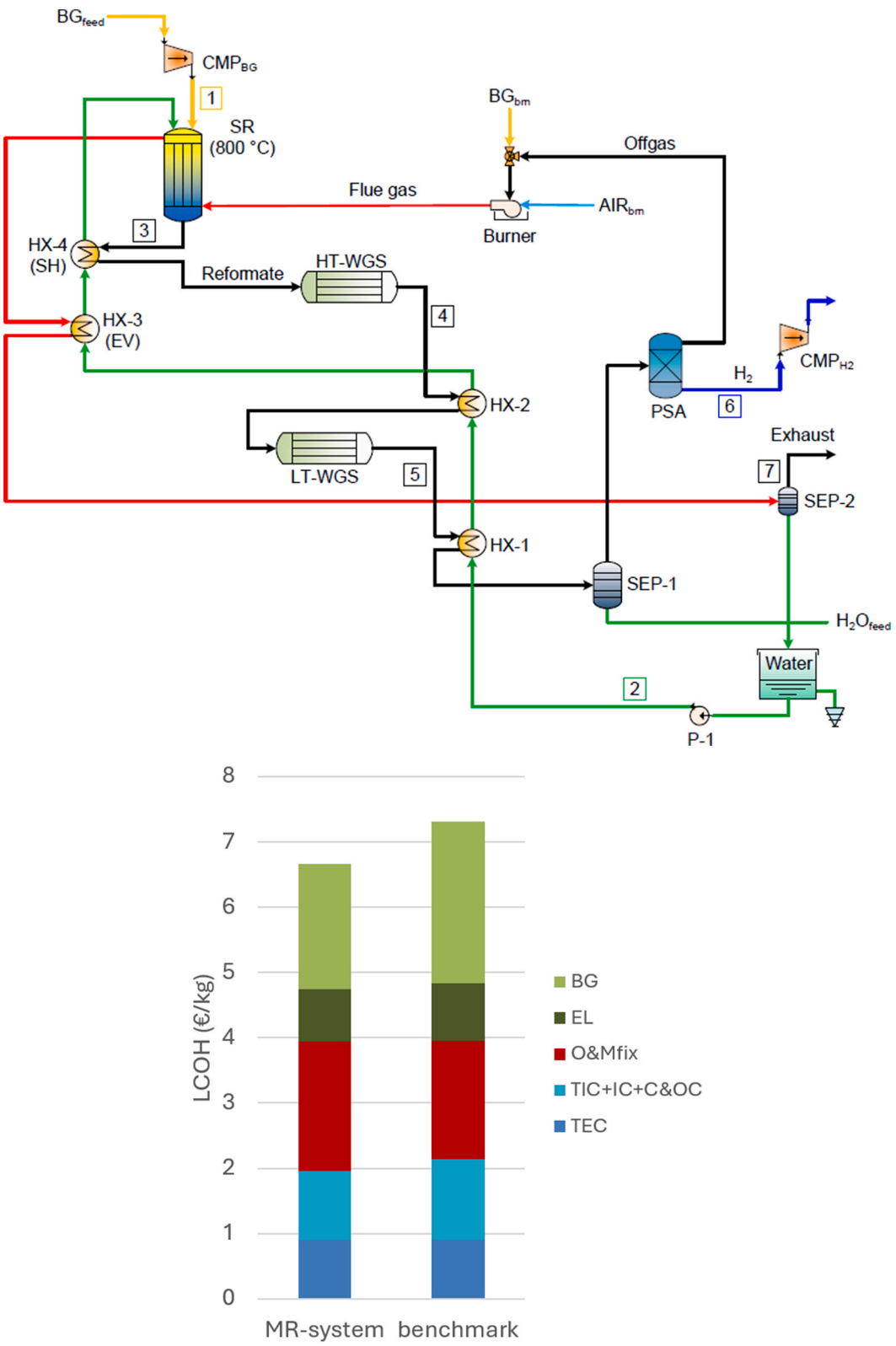

Fig. 11. On the top, layout of the benchmark plant, taken from Di Marcoberardino et al. [5]. On the bottom, LCOH comparison between design base-case with membrane reactor (this article) and the benchmark (with updated economic analysis) for production at 20 bar.

the components that process hydrogen (vacuum pump, compressor, economizer): due to uncertainty on their market prices, a factor of 5 has been considered in their cost estimation. Eventually labour cost is doubled. Costs assumptions for the sensitivity analysis are summarized in Table 9.

Results of the economic sensitivity are reported in Fig. 12: it is also reported the range of green hydrogen prices in 2022 of IEA [45], estimated in the range 1.5–12 USD/kg (about 1.4–11.1 €/kg) for different production technologies (solar PV, wind, nuclear). Equipment drives LCOH out of green hydrogen production range, but also the BG and

Table 9
Sensitivity analysis on process economics.

Parameter	Alias	Base	High value	High-LCOH (€/kg)
Biogas cost (€/Nm^3)	BG	0.2712	0.516	9.22
Electricity cost (€/kWh)	el	0.12	0.1893	8.11
Membranes cost (k€/m$_2$)	mem.s	5,5	55	10.34
Factor for H_2 components (−)	Equip.	1	5	13.72
Labour cost (k€/y)	Labour	30	60	8.45

membrane costs can notably influence the final hydrogen cost.

Beyond the variations in absolute values of LCOH, another interesting trend is to observe how these costs shift the optimum working point in terms of HRF-A_{mem}. For most of them (BG, electricity, labour, equipment costs), a variation in the specific cost only vertically shifts the LCOH curve in Fig. 8 towards higher values, without affecting the shape. Changing only membranes cost, however, has also an influence in the shape of the LCOH curve and therefore the conclusion that the best operating point is close to the limit for heat integration might not be valid anymore. Changing the membrane cost from 5.5 to 55 k€/m^2, the minimum is found at 2.7 m^2 instead of 2.87 m^2, corresponding to 135 membranes.

4.5. Increasing reactor temperature

The design conditions of the reactor have been set based on the state-of-the-art values and on previous analysis in similar plants. Among the investigated parameters, WHSV has been fixed to guarantee a near-equilibrium condition, where additional catalyst do not produce a sensible improvement in hydrogen production and HRF. SCR is tailored on the catalyst specifications, to guarantee a correct behaviour and avoid carbon formation. Vacuum pump pressure is in general beneficial to be kept at lowest value possible, and 0.1 bar was considered a good value for industrial size, while it would be difficult to go below.

Based on these considerations, the only variables which effect is interesting to investigate are reactor temperature and pressure. Reactor temperature is a key parameter. Higher temperatures allow higher conversions of methane and catalyst volume reduction, due to its higher activity. On the other hand, maximum operating temperature is limited by the operability and lifetime of the selected Pd-based membranes: calculations have been performed at 525 °C to show how small technological improvements in membrane manufacturing can improve overall performance. As can be seen in Fig. 13, minimum LCOH resulted 6.72 €/kg (vs 6.81 €/kg at 500 °C). System efficiency rose from 59.8% to 60.1%, HRF from 83% to 85.2%, given by the product of hydrogen recovery 95.3% (vs 95.6% at 500 °C) and methane conversion (89.5%, vs 86.8% at 500 °C). However, the major improvement is the 17% reduction of the required membrane area with a value of 2.375 m^2 (then 120 membranes), compared to 2.87 m^2 at 500 °C. This is particularly significant in case membrane cost and maintenance are higher than expected: in the high-cost membrane case (55 k€/m^2), the LCOH goes from 10.34 at 500 °C to 9.07 €/kg at 525 °C.

5. Conclusions

Membrane reactors are a promising technology for small-scale productions of green hydrogen from biogas. This technology is close to industrial maturity and more information about its behaviour is required to successfully predict its performance and to develop the scaling up.

In this article, two novelties compared to previous literature have been introduced. The first is the definition of generalized performance charts, which have as y-axis the hydrogen recovery factor and in the x-axis the hydrogen production per unit membrane area. In these charts, reactor performance - when temperature, pressure, the feed temperature, vacuum-side pressure and WHSV have been set – are summarized. All the possible working points lie on a single line, called generalized performance line. It is possible to move along the line by changing the ratio between biogas flow rate and membrane area. Each working point on the line can be obtained for different combinations of the membranes' length, pitch and the fluidization velocity. In general, for each point, it turned out to be convenient to work minimizing the membranes' pitch and maximizing membranes' length and consequently gas velocity, since a final total reactor volume results in reducing its costs and the amount of filler material.

The second novelty, that is based on the previous conclusion, is that the techno-economic assessment was generalized in terms of total membrane area in the reactor, without being bounded to a precise geometry. This generalization allowed to reduce the number of analyses required, compared to previous investigation in literature.

From the system point of view, the process was designed to produce 100 kg$_{H2}$/day. Design conditions were taken from state-of-the-art considerations and preliminary assessment of similar systems. Reactor temperature have been set to 500 °C, 0.1 bar at the vacuum side. SCR is 3 and WHSV 0.5 h^{-1}, to guarantee always near-equilibrium conditions.

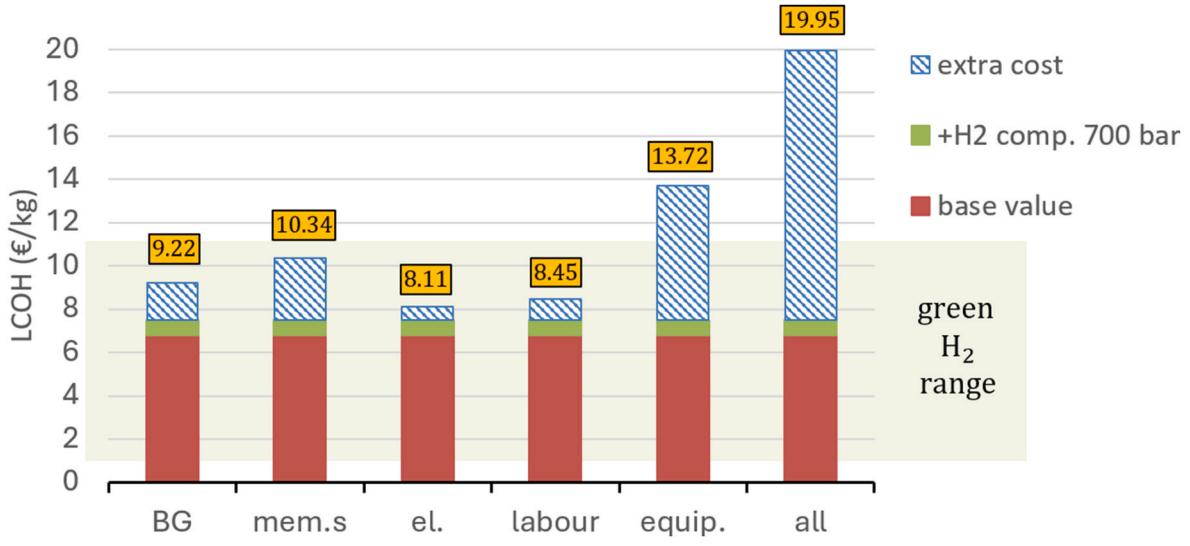

Fig. 12. Effect of costs uncertainties on LCOH. In dashed region, extra cost obtained using high-value for each variable.

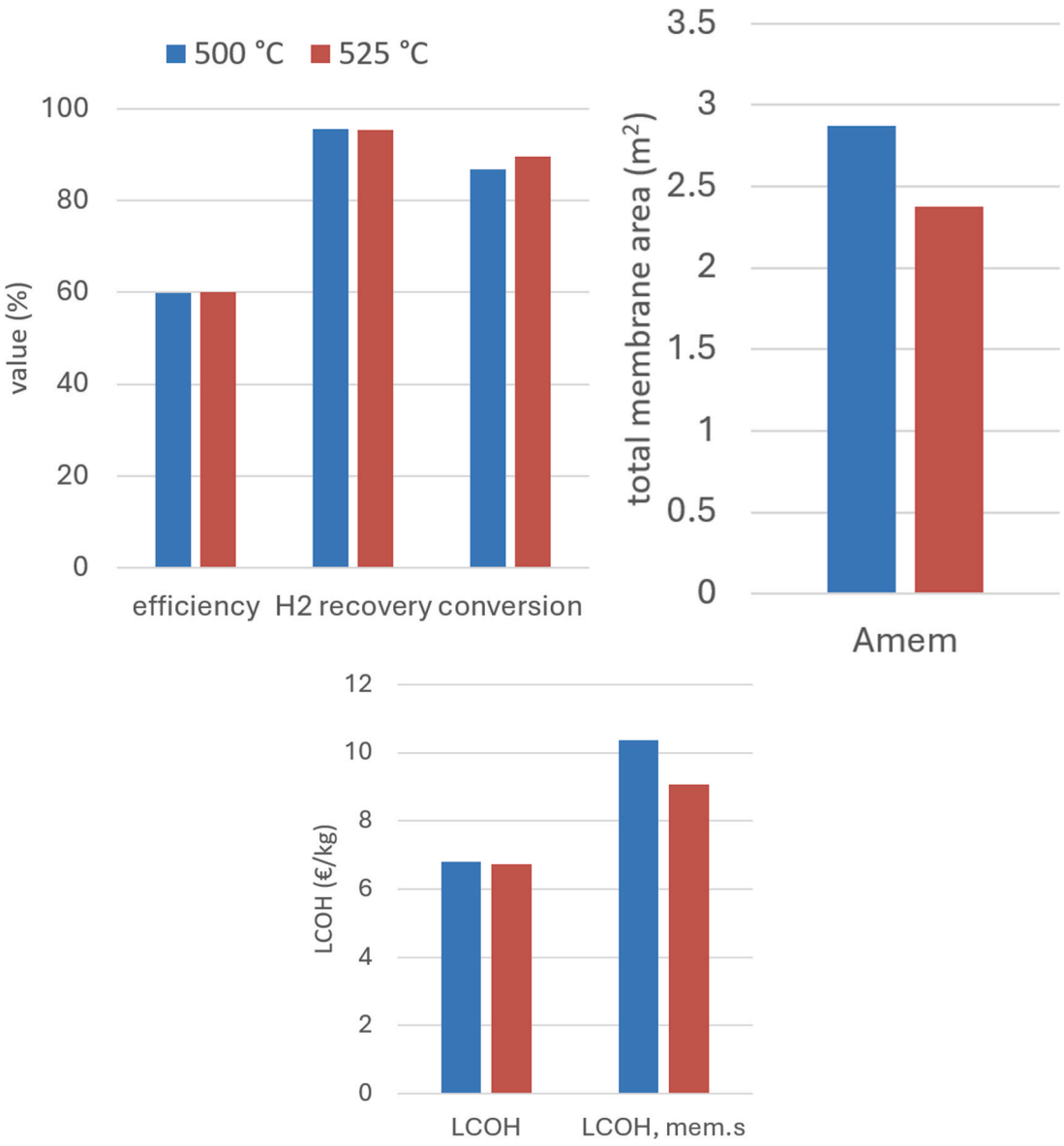

Fig. 13. comparison between system performance (efficiency), hydrogen recovery and methane conversion (which product gives the HRF), membrane area and LCOH at 500 °C and 525 °C. On the right, also the case with high membrane cost.

Reactor pressure have been variated in the range 9–18 bar: in this case, minimum LCOH resulted to be constant in that range, although the minimum shifts towards a lower membrane area as pressure increases. Costs are from one side reduced since membrane area is reduced but increased by additional requirements of electric energy for the compression. A value of 12 bar have been selected as design value.

In all analyses, membrane area has been variated to find the minimum LCOH in the trade off between higher HRF (lower biogas consumption) and higher membranes cost. The minimum in the design case turned out to be 6.65 €/kg, going up to 6.81 including average costs of filler and vessel, and up to 7.49 €/kg also including the hydrogen compressor at 700 bar. These values have been compared to the benchmark solution, based on obtaining the same hydrogen production by feeding biogas to a "conventional" process, made by an equilibrium reforming reactor followed by a PSA for hydrogen removal. For the production at 20 bar, MR-based system has an LCOH at 6.81 €/kg, while benchmark LCOH resulted 7.31 €/kg, due mainly to its lower hydrogen recovery.

Since some costs suffer from a certain level of uncertainty, a sensitivity analysis has been performed to assess their influence on hydrogen production cost. In general, most of the costs' variations (membranes, biogas, electric energy, labour) still allowed to obtain a LCOH inside the green hydrogen production range identified by IEA. This is the case considering all cost separately, but not if all costs are considered together at their top value. In that case, final cost could reach values up to 19.95 €/kg.

Finally, a simulation at 525 °C have been performed to investigate potential benefits of a temperature increase. Major conclusion was that higher temperatures allow us to reduce the membrane area, making them particularly interesting in case the Pd-based membrane price would be higher to what assumed in this analysis.

In conclusion, a generalized methodology has been provided to assess the performance of a membrane reactor for pure hydrogen production from autothermal biogas reforming, showing how MR-based solution is competitive against benchmark production route.

CRediT authorship contribution statement

Michele Ongis: Writing – original draft, Methodology, Investigation, Conceptualization. **Mattia Baiguini:** Writing – review & editing,

Visualization, Investigation, Formal analysis. **Gioele Di Marcoberardino:** Writing – review & editing, Methodology, Conceptualization. **Fausto Gallucci:** Writing – review & editing, Supervision. **Marco Binotti:** Writing – review & editing, Supervision, Methodology, Conceptualization.

Funding

This project has received funding from the European Union's Horizon 2020 Research and Innovation Program under grant agreement No. 869896 (MACBETH).

Declaration of competing interest

The authors declare that they have no known competing financial interests or personal relationships that could have appeared to influence the work reported in this paper.

Nomenclature

Parameter	Description	Unit
A_{mem}	Total membrane area	m^2
C	Gas concentration	mol/m^3
C_k	Cost of component k	k€
$C_{k.0}$	Reference cost of component k	k€
$C_{O\&M_{fix}}$	Fixed operation and maintenance cost	€/y
$C_{O\&M_{var}}$	Variable operation and maintenance cost	€/h
CCF	Capital charge factor	1/y
$CEPCI_y$	CEPCI index at year y	–
d	Membrane pitch	cm
d_m	Membrane diameter	cm
d_R	Reactor diameter	cm
f	Exponent in components cost equation	–
h_{eq}	Equivalent yearly hours of plant functioning	h/y
HRF	Hydrogen recovery factor	–
j_{H_2}	Hydrogen flux through the membrane	$kmol/(h\bullet m^2)$
k_m	Mass transfer coefficient	m/h
L_m	Membrane length	m
$LCOH$	Levelized cost of hydrogen	€/kg
LHV_i	Lower heating value of component i	MJ/kg
$\dot{m}_i$	Mass flow rate of component i	kg/s
n	Pressure exponent in permeation equation	–
$\dot{n}_i$	molar flow rate of component i	kmol/h
N_{mem}	Number of membranes	–
p_R	Reactor pressure	bar_a
p_p	Permeate-side pressure	bar_a
Pe	Membrane permeance	$kmol/(h\bullet m^2\bullet bar^{0.5})$
S_k	Size of plant component k	x
$S_{k.0}$	Reference size of plant component k	x
SCR	Ratio between moles of steam and moles of methane fed	–
T_R	Reactor temperature	°C
T_{feed}	Feed temperature	°C
TPC	Total plant cost	€
u	Superficial gas velocity in the reactor	m/s
u_{mf}	Minimum fluidization superficial gas velocity	m/s
$\dot{W}_{el}$	Electric power required by the auxiliaries	MW_{el}
Greek letters		
ΔT	Difference of temperature	x
η_{H2Ps}	System efficiency	–
$\eta_{el,ref}$	Reference value for electricity generation efficiency	–
Symbols		
$\%_{TIC}$	Percentage contribution of installation costs to TPC	–
$\%_{IC}$	Percentage contribution of indirect cost to TPC	–
$\%_{C\&OC}$	Percentage contribution of owner's and contingencies costs on TPC	–
Subscripts		
in	Parameter at the reactor/system inlet	
ox	Oxidated	
$perm$	Permeated	
y	Reference year	
$bulk$	Related to the bulk of the retentate	
m	Related to the conditions at membrane surface	
Acronyms		
BG	Biogas	
WGS	Water gas shift	
PSA	Pressure swing adsorption	
MR	Membrane reactor	
FBMR	Fluidized bed membrane reactor	
EU	European union	
MACBETH	Membranes and catalysts beyond economic and technological hurdles	
TRL	Technology readiness level	
ATR	AutoThermal reforming	

(*continued on next page*)

(*continued*)

Parameter	Description	Unit
1D	Mono-dimensional	
ACM	Aspen custom modeler	
HRF	Hydrogen recovery factor	
SCR	Steam-carbon-ratio	
LHV	Lower heating value	
ECO	Economizer	
EVA	Evaporator	
SH	Superheater	
KPI	Key performance indicator	
H2PS	Hydrogen production system	
LCOH	Levelized cost of hydrogen	
TPC	Total plant cost	
CCF	Capital charge factor	
O&M	Operation and maintenance	
TEC	Total equipment cost	
TIC	Total installation cost	
IC	Indirect cost	
C&OC	Owner's and contingencies costs	
UTS	Ultimate tensile strength	
ASME	American society of mechanical engineers	
CEPCI	Chemical engineering plant cost index	
WHSV	Weight hourly space velocity	
TEA	Techno-economic analysis	
IEA	International energy agency	

Appendix A. Supplementary data

Supplementary data to this article can be found online at https://doi.org/10.1016/j.ijhydene.2024.12.245.

References

[1] International Energy Agency. The Future of Hydrogen: seizing today's opportunities. IEA Publ; 2019. p. 203. https://www.iea.org/reports/the-future-of-hydrogen.

[2] Scarlat N, Dallemand JF, Fahl F. Biogas: developments and perspectives in Europe. Renew Energy 2018;129:457–72. https://doi.org/10.1016/j.renene.2018.03.006.

[3] International Energy Agency. Outlook for biogas and biomethane. Prospects for organic growth. World Energy Outlook Special Report 2020:93. https://www.iea.org/reports/outlook-for-biogas-and-biomethane-prospects-for-organic-growth.

[4] Guandalini G, Campanari S, Valenti G. Comparative assessment and safety issues in state-of-the-art hydrogen production technologies. Int J Hydrogen Energy 2016;41:18901–20. https://doi.org/10.1016/J.IJHYDENE.2016.08.015.

[5] Di Marcoberardino G, Vitali D, Spinelli F, Binotti M, Manzolini G. Green hydrogen production from raw biogas: a techno-economic investigation of conventional processes using pressure swing adsorption unit. Process 2018;6(6):19. https://doi.org/10.3390/PR6030019 (2018) 19.

[6] Gallucci F, Pacheco Tanaka DA, Medrano JA, Viviente Sole JL. Membrane reactors using metallic membranes. Elsevier Inc.; 2020. https://doi.org/10.1016/B978-0-12-818332-8.00010-7.

[7] Di Marcoberardino G, Binotti M, Manzolini G, Viviente JL, Arratibel A, Roses L, Gallucci F. Achievements of European projects on membrane reactor for hydrogen production. J Clean Prod 2017;161:1442–50. https://doi.org/10.1016/J.JCLEPRO.2017.05.122.

[8] Gallucci F, Fernandez E, Corengia P, van Sint Annaland M. Recent advances on membranes and membrane reactors for hydrogen production. Chem Eng Sci 2013;92:40–66. https://doi.org/10.1016/j.ces.2013.01.008.

[9] Arratibel A, Pacheco Tanaka A, Laso I, van Sint Annaland M, Gallucci F. Development of Pd-based double-skinned membranes for hydrogen production in fluidized bed membrane reactors. J Membr Sci 2018;550:536–44. https://doi.org/10.1016/J.MEMSCI.2017.10.064.

[10] Arratibel A, Medrano JA, Melendez J, Pacheco Tanaka DA, van Sint Annaland M, Gallucci F. Attrition-resistant membranes for fluidized-bed membrane reactors: double-skin membranes. J Membr Sci 2018;563:419–26. https://doi.org/10.1016/j.memsci.2018.06.012.

[11] MACBETH » Macbeth, (n.d.). https://www.macbeth-project.eu/(accessed January 1, 2023).

[12] Bellini S, Azzato G, Gallucci F, Caravella A. Mass transport in hydrogen permeation through Pd-based membranes. Elsevier Inc.; 2020. https://doi.org/10.1016/B978-0-12-818332-8.00003-X.

[13] Raimondi G, Greco G, Ongis M, D'Antuono G, Lanni D, Spazzafumo G. Techno-economical assessment for combined production of hydrogen, heat, and power from residual lignocellulosic agricultural biomass in huesca province (Spain). Energies 2024;17. https://doi.org/10.3390/en17040813.

[14] Ververs WJR, Arratibel A, Di Felice L, Gallucci F. A multi-layer model for double-skin Pd-based membranes: layer-by-layer parameter fitting. Int J Hydrogen Energy 2024;72:462–74. https://doi.org/10.1016/j.ijhydene.2024.05.225.

[15] Sheintuch M, German ED. Permeance inhibition due to reaction, coking and leakage of Pd membranes during methane steam reforming estimated from a micro-kinetic model. Chem Eng J 2021;411:128272. https://doi.org/10.1016/j.cej.2020.128272.

[16] Gallucci F. Modeling of membrane reactors. INC; 2022. https://doi.org/10.1016/B978-0-12-823659-8.00001-0.

[17] Gallucci F, Van Sintannaland M, Kuipers JAM. Theoretical comparison of packed bed and fluidized bed membrane reactors for methane reforming. Int J Hydrogen Energy 2010;35:7142–50. https://doi.org/10.1016/j.ijhydene.2010.02.050.

[18] Gallucci F, Basile A. Pd-Ag membrane reactor for steam reforming reactions: a comparison between different fuels. Int J Hydrogen Energy 2008;33:1671–87. https://doi.org/10.1016/j.ijhydene.2008.01.010.

[19] Brencio C, Di Felice L, Gallucci F. Fluidized bed membrane reactor for the direct dehydrogenation of propane: proof of concept. Membr 2022;12(12):1211. https://doi.org/10.3390/MEMBRANES12121211 (2022) 1211.

[20] Cechetto V, Di Felice L, Gutierrez Martinez R, Arratibel Plazaola A, Gallucci F. Ultra-pure hydrogen production via ammonia decomposition in a catalytic membrane reactor. Int J Hydrogen Energy 2022;47:21220–30. https://doi.org/10.1016/j.ijhydene.2022.04.240.

[21] Richard S, Ramirez A, Olivier P, Gallucci F. Techno-economic analysis of ammonia cracking for large scale power generation. Int J Hydrogen Energy 2024;71:571–87. https://doi.org/10.1016/j.ijhydene.2024.05.308.

[22] Richard S, Verde V, Kezibri N, Makhloufi C, Saker A, Gargiulo I, Gallucci F. Power-to-ammonia synthesis process with membrane reactors : techno- economic study. Int J Hydrogen Energy 2024;73:462–74. https://doi.org/10.1016/j.ijhydene.2024.06.041.

[23] Sjardin M, Damen KJ, Faaij APC. Techno-economic prospects of small-scale membrane reactors in a future hydrogen-fuelled transportation sector. Energy 2006;31:2523–55. https://doi.org/10.1016/J.ENERGY.2005.12.004.

[24] Di Marcoberardino G, Gallucci F, Manzolini G, van Sint Annaland M. Definition of validated membrane reactor model for 5 kW power output CHP system for different natural gas compositions. Int J Hydrogen Energy 2016;41:19141–53. https://doi.org/10.1016/J.IJHYDENE.2016.07.102.

[25] Di Marcoberardino G, Foresti S, Binotti M, Manzolini G. Potentiality of a biogas membrane reformer for decentralized hydrogen production. Chem. Eng. Process. - Process Intensif. 2018;129:131–41. https://doi.org/10.1016/J.CEP.2018.04.023.

[26] Ongis M, Di Marcoberardino G, Manzolini G, Gallucci F, Binotti M. Membrane reactors for green hydrogen production from biogas and biomethane: a techno-economic assessment. Int J Hydrogen Energy 2023;48:19580–95. https://doi.org/10.1016/j.ijhydene.2023.01.310.

[27] Spallina V, Pandolfo D, Battistella A, Romano MC, Van Sint Annaland M, Gallucci F. Techno-economic assessment of membrane assisted fluidized bed reactors for pure H2 production with CO2 capture. Energy Convers Manag 2016;120:257–73. https://doi.org/10.1016/J.ENCONMAN.2016.04.073.

[28] Bruni G, Rizzello C, Santucci A, Alique D, Incelli M, Tosti S. On the energy efficiency of hydrogen production processes via steam reforming using membrane reactors. Int J Hydrogen Energy 2019;44:988–99. https://doi.org/10.1016/j.ijhydene.2018.11.095.
[29] Foresti S, Di Marcoberardino G, Manzolini G, De Nooijer N, Gallucci F, van Sint Annaland M. A comprehensive model of a fluidized bed membrane reactor for small-scale hydrogen production. Chem. Eng. Process. - Process Intensif. 2018;127:136–44. https://doi.org/10.1016/j.cep.2018.01.018.
[30] Ongis M, Di Marcoberardino G, Baiguini M, Gallucci F, Binotti M. Optimization of small-scale hydrogen production with membrane reactors. Membranes 2023;13. https://doi.org/10.3390/membranes13030331.
[31] de Nooijer N, Gallucci F, Pellizzari E, Melendez J, Pacheco Tanaka DA, Manzolini G, van Sint Annaland M. On concentration polarisation in a fluidized bed membrane reactor for biogas steam reforming: modelling and experimental validation. Chem Eng J 2018;348:232–43. https://doi.org/10.1016/j.cej.2018.04.205.
[32] De Nooijer N. Reforming towards renewable hydrogen: biogas steam reforming in a fluidized bed membrane reactor. 2022.
[33] Di Marcoberardino G, Vitali D, Spinelli F, Binotti M, Manzolini G. Green hydrogen production from raw biogas: a techno-economic investigation of conventional processes using pressure swing adsorption unit. Processes 2018;6. https://doi.org/10.3390/pr6030019.
[34] Di Marcoberardino G, Foresti S, Binotti M, Manzolini G. Potentiality of a biogas membrane reformer for decentralized hydrogen production. Chem. Eng. Process. - Process Intensif. 2018;129:131–41. https://doi.org/10.1016/j.cep.2018.04.023.
[35] American Society of Mechanical Engineers, American Society of Mechanical Engineers. Boiler and pressure vessel code, section VIII - rules for construction of pressure vessels. Am Soc Mech Eng 2021:804. https://www.asme.org/codes-standards/find-codes-standards/bpvc-viii-1-bpvc-section-viii-rules-construction-pressure-vessels-division-1. [Accessed 3 February 2023].
[36] zirconia powder, low cost grade, (n.d.). http://www.inframat.com/products/40R-0803CF.htm (accessed February 3, 2023).
[37] Rhodium Price Chart: Check Live & Historical Rhodium Spot Prices, (n.d.). https://www.moneymetals.com/rhodium-price (accessed February 3, 2023).
[38] Nordio M, Melendez J, van Sint Annaland M, Pacheco Tanaka DA, Llosa Tanco M, Gallucci F. Comparison between carbon molecular sieve and Pd-Ag membranes in H2-CH4 separation at high pressure. Int J Hydrogen Energy 2020;45:28876–92. https://doi.org/10.1016/j.ijhydene.2020.07.191.
[39] R. Smith, Chemical process design and integration, (n.d.).
[40] Nordio M, Wassie SA, Van Sint Annaland M, Pacheco Tanaka DA, Viviente Sole JL, Gallucci F. Techno-economic evaluation on a hybrid technology for low hydrogen concentration separation and purification from natural gas grid. Int J Hydrogen Energy 2021;46:23417–35. https://doi.org/10.1016/J.IJHYDENE.2020.05.009.
[41] ToweringSkills. CEPCI index. https://toweringskills.com/financial-analysis/cost-indices/; 2024.
[42] Voncken RJW, Roghair I, van Sint Annaland M. A numerical study on concentration polarization in 3D cylindrical fluidized beds with vertically immersed membranes. Chem Eng Sci 2019;205:299–318. https://doi.org/10.1016/j.ces.2019.05.010.
[43] ARERA - Prezzi finali dell'energia elettrica per i consumatori industriali - Ue a Area euro, (n.d.). https://www.arera.it/it/dati/eepcfr2.htm (accessed December 13, 2022).
[44] Ververs WJR, Ongis M, Arratibel A, Di Felice L, Gallucci F. On the modeling of external mass transfer phenomena in Pd-based membrane separations. Int J Hydrogen Energy 2024;71:1121–33. https://doi.org/10.1016/j.ijhydene.2024.04.337.
[45] I. - International Energy Agency. Global hydrogen review 2023. Glob. Hydrog. Rev. 2023;2023. https://doi.org/10.1787/cb2635f6-en.